Measurement of the Bottom-Quark Production Cross Section in 800 GeV/c Proton-Gold Collisions

D. M. Jansen,[1] M. H. Schub,[2,*] C. S. Mishra,[3] P. M. Ho,[4] C. N. Brown,[3] T. A. Carey,[1] Y. C. Chen,[5,9] R. Childers,[6] W. E. Cooper,[3] C. W. Darden,[6] G. Gidal,[4] K. N. Gounder,[3,†] L. D. Isenhower,[7] R. G. Jeppesen,[1,‡] D. M. Kaplan,[8,§] J. S. Kapustinsky,[1] G. C. Kiang,[9] M. S. Kowitt,[4,‖] D. W. Lane,[1,¶] L. M. Lederman,[2,§] M. J. Leitch,[1] J. W. Lillberg,[1] W. R. Luebke,[8,§] K. B. Luk,[4] P. L. McGaughey,[1] J. M. Moss,[1] J. C. Peng,[1] R. S. Preston,[8] D. Pripstein,[4] J. Sa,[8] M. E. Sadler,[7] R. Schnathorst,[7,**] V. Tanikella,[8] P. K. Teng,[9] and J. R. Wilson[6]

[1]*Los Alamos National Laboratory, Los Alamos, New Mexico 87545*
[2]*University of Chicago, Chicago, Illinois 60637*
[3]*Fermi National Accelerator Laboratory, Batavia, Illinois 60510*
[4]*Lawrence Berkeley Laboratory and University of California, Berkeley, California 94720*
[5]*National Cheng Kung University, Tainan, Taiwan, Republic of China*
[6]*University of South Carolina, Columbia, South Carolina 29208*
[7]*Abilene Christian University, Abilene, Texas 79699*
[8]*Northern Illinois University, DeKalb, Illinois 60115*
[9]*Institute of Physics, Academia Sinica, Taipei, Taiwan, Republic of China*

(Received 30 November 1994; revised manuscript received 11 January 1995)

Using a silicon-microstrip detector array to identify secondary vertices, we have observed $b \to J/\psi \to \mu^+\mu^-$ decays in 800 GeV/c proton-gold interactions. The doubly differential cross section for J/ψ mesons originating from b-quark decays, assuming linear dependence on nucleon number, is $d^2\sigma/dx_F\,dp_T^2 = 107 \pm 28 \pm 19$ [pb/(GeV/c)^2]/nucleon at $x_F = 0.05$ and $p_T = 1$ GeV/c. This measurement is compared to next-to-leading-order QCD predictions. The integrated b-quark production cross section, obtained by extrapolation over all x_F and p_T, is $\sigma(pN \to b\bar{b} + X) = 5.7 \pm 1.5 \pm 1.3$ nb/nucleon.

PACS numbers: 13.85.Ni, 25.38.Qk, 24.85.+p, 25.40.Ve

We report the first measurement of the b-quark production cross section in proton-nucleus interactions. Production of b quarks was observed via inclusive $b \to J/\psi \to \mu^+\mu^-$ decays. Previous measurements of the b-quark production cross section are available from the CERN [1] and Fermilab [2–4] $p\bar{p}$ colliders, and from fixed-target experiments using pion beams [5]. These data have been compared to recent next-to-leading-order calculations for b-quark production [6]. Our measurement provides proton-induced data, at a smaller $\sqrt{s}$ than the colliders, which can be used to test the QCD predictions.

The experiment was performed at Fermilab using the E605 spectrometer [7]. The spectrometer can detect pairs of charged particles, has good mass resolution, and can handle high interaction rates. To provide sufficient resolution in vertex position to distinguish the decays of b hadrons from the copious "prompt" (i.e., originating at the primary interaction vertex) backgrounds, we added an array of 16 silicon-microstrip detectors (SMDs) downstream of the target. We also increased the data-acquisition capacity by an order of magnitude (to 50 Mbytes/spill) and replaced the multiwire proportional chambers with small-cell drift chambers.

An 800 GeV/c primary proton beam was incident along the z axis upon a rectangular gold target 5 cm $\times$ 0.2 mm $\times$ 3 mm ($\Delta x \times \Delta y \times \Delta z$) in size, where the target center defined the origin of the coordinate system and the y axis was in the vertical direction. Because of the wirelike shape of the target, the primary interaction vertex had well-localized y and z coordinates which need not be reconstructed. The high laboratory momenta ($\approx$150 GeV/c) of b hadrons within our acceptance imply that the production and decay vertices are separated by an average distance of 1.3 cm. Vacuum extended from far upstream of the target to a 130-μm-thick titanium window located 28 cm downstream of the target, ensuring that interactions in windows or in air could not be confused with b-hadron decays.

The SMDs were 5 cm $\times$ 5 cm $\times$ 300 μm single-sided detectors with a 50-μm strip pitch. They were situated 37 to 94 cm downstream of the target, in an enclosure filled with helium gas cooled to 10 °C, and grouped into an upper and a lower arm. Each arm consisted of four y-view detectors with strips lying horizontally and four stereo-view detectors with strips tilted $\pm 5°$ from the x axis. The angular coverage of the instrumented strips, $20 \leq |\theta_y| \leq 60$ mr, matched the acceptance of the magnetic spectrometer. Signals from 8544 strips were processed by Fermilab-Penn preamplifiers [8] and LBL discriminators [9] followed by latches. The resolution in decay distance provided by the SMD arrays, $\approx$0.7 mm rms, was confirmed by reconstructing the decays of D^0 mesons produced in 800 GeV/c proton-nucleus interactions [10]. The close agreement of the D^0 lifetime obtained there with the world average [11] further confirms our understanding of the SMD calibration and efficiency.

 0031-9007/95/74(16)/3118(4)$06.00

The dimuon data were collected with approximately 3×10^{10} protons on target per 20 s beam spill, corresponding to a 50 MHz interaction rate. The magnet current was set to optimize acceptance for $J/\psi \rightarrow \mu^+\mu^-$ decays. The dimuon trigger required that the hit patterns in three hodoscope stations and in the muon counters be consistent with a $\mu^+\mu^-$ pair originating from the target region. To select muons passing through the apertures of the SMD arms, signals from a pair of scintillation counters, one situated behind each arm, were also required.

The event reconstruction requires identified muons with matching track segments in the SMD arrays. Muon tracks are first identified using information from the three drift-chamber stations, the muon station, and the calorimeter. Each muon track is then traced through the magnet to the target center, and roads are defined in the SMD arrays around the projected track positions. The matching silicon track segment is searched for using only the hits within the roads. Events are required to contain at least one pair of opposite-sign muons with valid SMD track segments. Requirements on the distance of closest approach between the two SMD tracks and on the x and y positions of the reconstructed vertex are then applied. An event cleanliness cut, requiring that the average hit multiplicity within the SMD roads be less than 7, is also applied. This cut removes approximately 10% of the dimuon data for which there is an increased probability of incorrectly reconstructing the SMD tracks. The observed performance of the SMD arrays is well reproduced by a detailed Monte Carlo simulation.

Figure 1 shows the dimuon invariant-mass spectrum. The J/ψ and ψ' resonances are clearly observed above a continuum. As verified by Monte Carlo simulation, the observed mass resolution is dominated by multiple scattering effects in the target. The continuum is attributed to a combination of π and K decays in flight, the Drell-Yan process, and semileptonic decays of heavy quarks. The differential J/ψ cross section determined using these data is very similar to CERN ISR results obtained at $\sqrt{s} = 52$ and 63 GeV [12] and is consistent with our measurements made at large x_F [13]. More details on the J/ψ and ψ' results are presented in a separate publication [14].

Figure 2(a) shows a scatter plot of the y coordinate (y_v) versus the z coordinate (z_v) of the reconstructed vertex

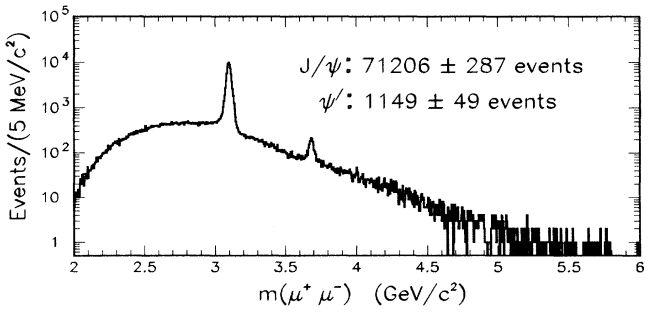

FIG. 1. Dimuon invariant-mass distribution.

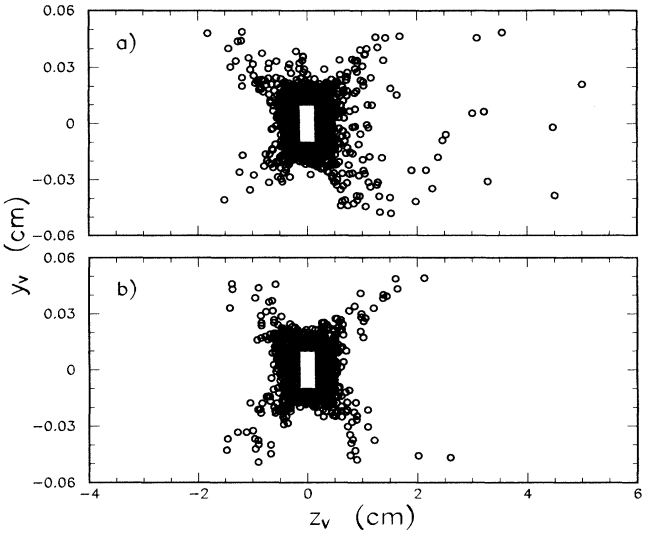

FIG. 2. Scatter plot of y_v vs z_v for all dimuon events in a 60 MeV/c^2 bin centered on the J/ψ peak: (a) data, (b) twice the number of prompt-J/ψ Monte Carlo events. Event vertices that lie within the rectangular wire target are not displayed.

for all dimuon events in a 60 MeV/c^2 bin centered on the J/ψ peak. This bin width is ± 3 standard deviations of the mass resolution for events in which the J/ψ decays downstream of the target. Figure 2(b) shows the same for twice the number of prompt-J/ψ Monte Carlo events. The diagonal bands arise from events in which one muon track points approximately to the target while the other does not. These events, fewer than 1% of the total, can originate from incorrect SMD reconstruction on one of the two arms, or, in the data, from semileptonic decays of heavy quarks. Such events are eliminated by the impact-parameter cuts described below. Compared to the events with $z_v < 0$, there is a clear excess of events in Fig. 2(a) in which the pair vertex is downstream of the target and outside of the diagonal bands. These events are evidence for the $b \rightarrow J/\psi \rightarrow \mu^+\mu^-$ process. The lack of such events in Fig. 2(b) confirms that they are not due to biases in the analysis code. Within the limited statistics of our sample, we have verified that the lifetime distribution of the downstream events is consistent with the measured lifetime [11] of b hadrons.

To select downstream $b \rightarrow J/\psi \rightarrow \mu^+\mu^-$ decays, cuts on the z_v of the muon pair and on the impact parameter of each muon track are applied. The impact parameters δ_i ($i = 1, 2$) are defined as the vertical distances between the muon tracks and the target center. The impact parameter requirements ensure that neither the μ^+ nor the μ^- track points to the target. Figure 3 shows the dimuon mass spectra for various z_v and impact parameter cuts. For each pair of figures, two mass spectra, one with downstream vertices ($z_v > 0$) and the other with upstream vertices ($z_v < 0$), are shown. The spectra with $z_v < 0$ provide a means to evaluate the contributions from the tails of the

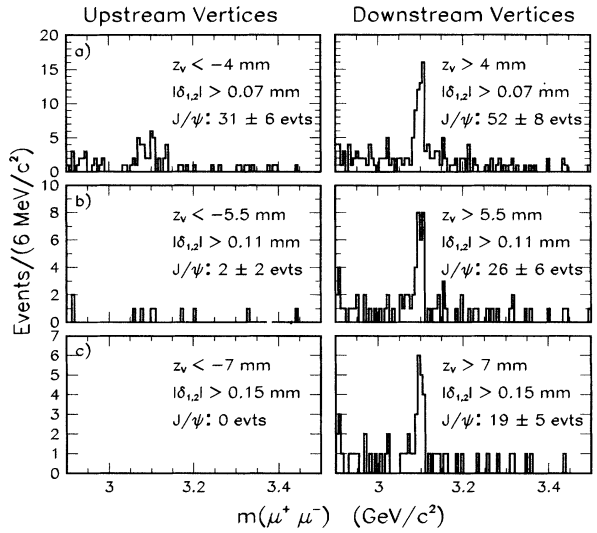

FIG. 3. Dimuon invariant-mass distributions for successively tighter cuts on z_v and on the absolute values of the impact parameters of the two muon tracks $|\delta_{1,2}|$.

prompt-J/ψ z_v distribution. The J/ψ peak is clearly seen in all three plots with $z_v > 0$. In contrast, the J/ψ yields in plots with $z_v < 0$ drop rapidly to zero as the vertex cuts are tightened [Figs. 3(b) and 3(c)]. We attribute the net excess of J/ψ events with downstream vertices to the $b \to J/\psi$ process.

The spectrometer acceptance and analysis efficiency have been determined using a detailed Monte Carlo program. The program simulates multiple scattering and detector inefficiencies and uses real event data to generate realistic noise hits in the detectors. To simulate production of b quarks and the decay $b \to J/\psi \to \mu^+\mu^-$ we use the following model: (1) the next-to-leading-order calculation by Mangano, Nason, and Ridolfi [6] is used to generate the x_F and p_T distributions of the b quark; (2) intrinsic transverse momentum is simulated with Gaussian distributions which give $\langle k_T^2 \rangle = 0.5$ (GeV/c)^2 [15]; (3) b-quark fragmentation is modeled using the Peterson function [16], with $\epsilon = 0.006 \pm 0.002$ as determined from e^+e^- annihilation [17]; (4) we use 1.537 ± 0.021 ps [11] as the average b-hadron lifetime; (5) since a b-quark fragments dominantly into a B_d or B_u meson, we use a distribution from the CLEO Collaboration [18] to simulate the momentum of J/ψ mesons originating from b-hadron decays; (6) a decay-angle distribution $1 - \lambda\cos^2\theta$, with $\lambda = 0.436 \pm 0.115$ [18], is used to simulate the J/ψ polarization.

The doubly differential cross section, averaged over our bin in J/ψ x_F and p_T ($0 < x_F < 0.1$, $p_T < 2$ GeV/c), for J/ψ mesons originating from b quarks is given by

$$\left\langle \frac{d^2\sigma}{dx_F\, dp_T^2} \right\rangle = \frac{N_{J/\psi}}{\Delta x_F\, \Delta p_T^2\, \eta\varepsilon \mathcal{L}\, A^\alpha B(J/\psi \to \mu^+\mu^-)},$$

where $N_{J/\psi}$ is the 19 ± 5 events shown in Fig. 3(c), $\Delta x_F \Delta p_T^2$ is the bin size, $\eta\varepsilon$ is the product of acceptance and efficiency, $\mathcal{L}$ is the integrated luminosity, $B(J/\psi \to \mu^+\mu^-) = (5.97 \pm 0.25)\%$ [11], and an atomic-weight (A) dependence of the form A^α is assumed. We assume $\alpha = 1$ for b-hadron production since recent experiments have shown no nuclear suppression of D-meson production [10]. By basing our cross section on the sample of Fig. 3(c) we avoid any uncertainties in the subtraction of upstream background and obtain optimal statistical significance. To minimize the systematic uncertainty due to changes in running conditions, we have chosen a subsample containing $(4.87 \pm 0.09)\%$ of the observed prompt-J/ψ events for careful study. For the subsample, $\eta\varepsilon = (0.285 \pm 0.036)\%$ and the luminosity is (0.853 ± 0.092) pb^{-1}. We normalize the rest of the data to this subsample under the assumption (verified by efficiency studies and Monte Carlo simulation) that the ratio of $b \to J/\psi$ to prompt-J/ψ event yields is independent of trigger and efficiency variations. We thus obtain $\langle d^2\sigma/dx_F\, dp_T^2 \rangle = 81 \pm 21 \pm 15$ [pb/(GeV/c)^2]/nucleon in the x_F, p_T bin given above. Within errors the cross section is stable as we vary our vertex cuts. A separate analysis using a different SMD track reconstruction program has also yielded a consistent result. The main systematic errors are the uncertainties in luminosity (±11%), efficiency (±10%), b-quark production, hadronization, and decay models (±8%), fitting of the mass spectrum (±5%), and J/ψ branching ratio (±4%).

To compare with theory we interpolate the average cross section to the point $x_F = 0.05$ and $p_T = 1$ GeV/c. Using the model of $b \to J/\psi$ production and decay described above, we find that the interpolated cross section is 1.32 times the average cross section (i.e., $107 \pm 28 \pm 19$ [pb/(GeV/c)^2] /nucleon) and that the interpolation has negligible systematic uncertainty. Figure 4 compares the interpolated cross section with representative predictions of the model. The predictions contain substantial uncertainties due to choices for the b-quark mass (37% decrease at our x_F and p_T as m_b varies from 4.75 to 5.00 GeV/c^2), the QCD renormalization scale (45% decrease as μ varies from $\sqrt{m_b^2 + p_T^2}$ to $2\sqrt{m_b^2 + p_T^2}$), and the choice of parton distribution functions (±30% variation with respect to the MRS D0 [19] set). The solid curve in Fig. 4 is based on the same assumptions as used recently by the CDF [3] and D0 [4] Collaborations. Compared to this prediction, our measurement is a factor of 2 low, while theirs are high by a similar factor. While the sensitivities of the predictions to the model assumptions differ at $\sqrt{s} = 1.8$ TeV and at fixed-target energies, within the framework of our next-to-leading-order QCD model, we have been unable to find a set of assumptions consistent with both our measurement and those of CDF and D0.

Using the relatively stable shapes predicted by our model to extrapolate over all x_F and p_T, and using $B(b\bar{b} \to J/\psi + X) = (2.60 \pm 0.34)\%$, which is twice the inclusive branching ratio for $B \to J/\psi + X$ [11], we derive a total cross section for producing a $b\bar{b}$ pair $\sigma(pN \to b\bar{b} + X) = 5.7 \pm 1.5 \pm 1.3$ nb/nucleon. As in the differential cross

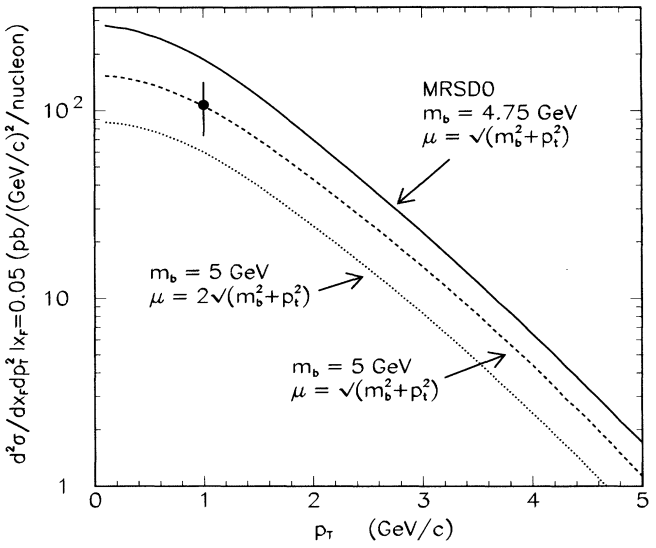

FIG. 4. $d^2\sigma/dx_F\,dp_T^2$ for J/ψ mesons originating from b-quark decays compared to predictions. The predictions, derived from the $b\bar{b}$ calculations described in Ref. [6] and our model of $b \rightarrow J/\psi$ decays, are shown for various values of the b-quark mass and the QCD renormalization scale μ.

section given above, this is approximately one-half of the central theoretical prediction.

This work was supported by the U.S. Department of Energy and the National Science Foundation. K. B. L. was partially supported by a DOE OJI award and an Alfred P. Sloan fellowship. Y. C. C., G. C. K., and P. K. T. were supported by the National Science Council of the Republic of China. We thank the Fermilab staff for their support and M. L. Mangano for valuable discussions.

*Present address: School of Physics and Astronomy, University of Minnesota, Minneapolis, MN 55455.
†Present address: Department of Physics, University of Mississippi, University, MS 38677.
‡Present address: Science Applications International Corp., 2950 Patick Henry Drive, Santa Clara, CA 95054.
§Present address: Department of Physics, Illinois Institute of Technology, Chicago, IL 60616.
‖Present address: NASA/Goddard Space Flight Center, Greenbelt, MD 20771.
¶Present address: Department of Physics, Iowa State University, Ames, IA 50011.
**Present address: Department of Physics, Purdue University, Lafayette, IN 47907.

[1] C. Albajar *et al.*, Phys. Lett. B **256**, 121 (1991).
[2] F. Abe *et al.*, Phys. Rev. Lett. **69**, 3704 (1992); M. Mangano *et al.*, Nucl. Instrum. Methods A **333**, 57 (1993).
[3] F. Abe *et al.*, Fermilab Report No. Fermilab-Conf-94/136-E; see also F. Abe *et al.*, Phys. Rev. D **50**, 4252 (1994), and references therein.
[4] S. Abachi *et al.*, Phys. Rev. Lett. (to be published).
[5] J. P. Albanese *et al.*, Phys. Lett. B **158**, 186 (1985); M. G. Catanesi *et al.*, *ibid.* **231**, 328 (1989); K. Kodama *et al.*, *ibid.* **303**, 359 (1993); R. Jesik *et al.*, Phys. Rev. Lett. **74**, 495 (1995).
[6] P. Nason, S. Dawson, and R. K. Ellis, Nucl. Phys. **B303**, 607 (1988); M. Mangano, P. Nason, and G. Ridolfi, Nucl. Phys. **B405**, 507 (1993).
[7] J. A. Crittenden *et al.*, Phys. Rev. D **34**, 2584 (1986).
[8] R. J. Yarema and T. Zimmerman, IEEE Trans. Nucl. Sci. **37**, 430 (1990); T. Zimmerman, *ibid.* **37**, 439 (1990).
[9] B. T. Turko *et al.*, IEEE Trans. Nucl. Sci. **39**, 758 (1992).
[10] M. J. Leitch *et al.*, Phys. Rev. Lett. **72**, 2542 (1994).
[11] Particle Data Group, L. Montanet *et al.*, Phys. Rev. D **50**, 1173 (1994).
[12] A. G. Clark *et al.*, Nucl. Phys. **B142**, 29 (1978); L. Lyons, Prog. Part. Phys. **7**, 169 (1981).
[13] M. S. Kowitt *et al.*, Phys. Rev. Lett. **72**, 1318 (1994).
[14] M. H. Schub *et al.* (present collaboration), "J/ψ and ψ' Production in 800 GeV/c Proton-Gold Collisions" (to be published).
[15] J. Chay, S. D. Ellis, and W. J. Stirling, Phys. Rev. D **45**, 46 (1992).
[16] C. Peterson *et al.*, Phys. Rev. D **27**, 105 (1983).
[17] J. Chrin, Z. Phys. C **36**, 165 (1987); D. Decamp *et al.*, Phys. Lett. B **244**, 551 (1990). This is also the value of ϵ used in Refs. [3] and [4].
[18] CLEO Collaboration, D. Besson *et al.* (private communication).
[19] A. D. Martin, W. J. Stirling, and R. G. Roberts, Phys. Lett. B **306**, 145 (1993).